

#### Central European Journal of Chemistry

# Noncovalent effects in the coordination and assembling of the[Fe(bpca)<sub>2</sub>][Er(NO<sub>3</sub>)<sub>3</sub>(H<sub>2</sub>O)<sub>4</sub>]NO<sub>3</sub> system

#### Research Article

Marilena Ferbinteanu<sup>1\*</sup>, Alina Zaharia<sup>1</sup>, Mihai A. Gîrțu<sup>2</sup>, Fanica Cimpoesu<sup>3</sup>

<sup>1</sup>Inorganic Chemistry Department, Faculty of Chemistry, University of Bucharest, Bucharest 020462, Romania

<sup>2</sup>Department of Physics, Ovidius University of Constanța, Constanța 900527, Romania

<sup>3</sup>Institute of Physical Chemistry, Bucharest 060021, Romania

Received 3 December 2009; Accepted 2 January 2010

Abstract: In this work we perform a detailed analysis of the non-covalent effects that build the lattice of the [Fe(bpca)<sub>2</sub>][Er(NO<sub>3</sub>)<sub>3</sub>(H<sub>2</sub>O)4]NO<sub>3</sub> compound, made of cationic d units [Fe(bpca)<sub>2</sub>] +,(where Hbpca is bis(2-pyridilcarbonyl)amine), neutral f complexes [Er(NO<sub>3</sub>)<sub>3</sub>(H<sub>2</sub>O)<sub>4</sub>], and the NO3- counter-ion. All these units are interlinked by hydrogen bonds, their assembling benefiting also from electrostatic effects. A particularly interesting sub-ensemble of the crystal is the linear chain formed by the lanthanide units. Going beyond the usual qualitative description of the supramolecular assembling, we performed electron structure calculations on appropriate models related to the experimental structures. The formation energies of d and f coordination bonds are estimated in semi-quantitative manner, being compared with the intermolecular ones, due to hydrogen bonding and dipolar interactions.

Keywords: Lanthanide chemistry • Supramolecular assembling • Bpca ligand • DFT calculations • Energy decomposition analysis.

© Versita Sp. z o.o.

## 1. Introduction

This work, placed in the general frame of lanthanide chemistry [1-3], belongs to a series of investigations exploiting the capability of the negatively charged bpca ligand (Hbpca=bis(2-pyridilcarbonyl)amine) to be tentatively used for the building of d-f complexes [4-6]. The planar ligand is ambident, showing a tridentate side with pyridine- and anionic amide- type nitrogen donor set and a bidentate dicarbonylic one. The N-type coordination is appropriate for binding d metal ions, while the O-type one is in principle accessible for binding oxofile lanthanide ions, as it is the case of the previously reported Fe-Dy dimer [4]. However, in certain cases the dicarbonylic chelators remains unused, the complexes consisting of d and f units that are not mutually connected. Such an example was previously discussed [5] for the case of a complex cation-complex anion type d-f coordination compound [Fe(bpca)<sub>a</sub>]

[Er(NO<sub>3</sub>)<sub>4</sub>(H<sub>2</sub>O)<sub>2</sub>] that showed independent [Fe(bpca)<sub>2</sub>]<sup>+</sup> moieties, while the lanthanide units were assembled in dimers [Er(NO<sub>3</sub>)<sub>4</sub>(H<sub>2</sub>O)<sub>2</sub>]<sub>2</sub><sup>2</sup>. The actual system shows a further structural variation since, while the [Fe(bpca)<sub>2</sub>]<sup>+</sup> complexes are isolated units, the nominal counter ion being simply a nitrate unit, the lanthanide complexes are neutral and assembled in extended chains. The nitrate counter ion is involved also in the hydrogen bonding along the lanthanide chain. In this work we focus on the description of the assembling, with electron structure details, the magnetism of this system being reported previously [6].

The lanthanide systems are a subject of enhanced interest and numerous recent studies [7-12] with focus on their magnetic properties, which are promising for the building of nano-scale magnets [13-15]. The complicate structure-properties relationships of lanthanides makes their coordination chemistry a challenging open field that offers case studies serving to draw new magneto-structural correlations or thumb rules for the

supramolecular assembling. To be distinguished from prototypic supramolecular chemistry, dealing with the packing of rather stable organic or d-type molecular units, the lanthanide complexes bring the issue of the relative floppiness of their own molecular structure [16-17]. This is due to the fact that the bonding of the coordination complexes is practically of noncovalent, merely ionic, nature [18]. Therefore, without the covalent-type feature of directed bonds the positions of the ligands on the coordination sphere are more flexible, a feature favoring the versatility during the supramolecular and lattice packing. We will get a deeper insight in the causal determination of such effects, using [Fe(bpca)<sub>2</sub>] [Er(NO<sub>3</sub>)<sub>3</sub>(H<sub>2</sub>O)<sub>4</sub>]•NO<sub>3</sub>•H<sub>2</sub>O as case study.

# 2. Experimental Procedure

#### 2.1 Materials

The synthesis and basic crystallographic data for the complex  $[Fe(bpca)_2][Er(NO_3)_3(H_2O)_4] \cdot NO_3 \cdot H_2O$  were described in a previous paper, dedicated to its magnetic properties [6]. Experimental crystallographic data were used for the detailed structural analysis of the noncovalent interaction in the lanthanide assemblies.

#### 2.2 Electronic structure calculations

The Density Functional Theory (DFT) calculations were done with the ADF code (Amsterdam Density Functional) [19-21]. The lanthanide complexes show non-aufbau electron structure, with partly filled f shell below many doubly occupied MOs belonging to the ligands. Such calculations cannot be done in a regular manner, this approach facing severe convergence problems. However, as we proved previously [5] for the calculation of the association energy and ignoring the topics strictly due to the f shell, such as magnetism, the diamagnetic Lu(III) ions can be reasonably used as surrogates of actual lanthanide ions in the molecular models. This is possible because the f shell is well confined inside the lanthanide ion and does not contribute to the bonding. The calculations were done on [Lu(H<sub>2</sub>O)<sub>4</sub>(NO<sub>3</sub>)<sub>3</sub>] models taken at experimental geometry of the crystallographic nonequivalent [Er(H<sub>2</sub>O)<sub>4</sub>(NO<sub>3</sub>)<sub>3</sub>] units. The triple zeta polarized (TZP) basis set and the Becke-Perdew gradient corrected functional were used [22-24].

## 3. Results and Discussion

#### 3.1 Structure description

The crystal shows a triclinic cell with P-1 space group, i.e. having the inversion as sole lattice symmetry. There are three crystallographic nonequivalent species for each constituting moiety, the d cation, the nitrate anion and the f neutral molecule. The d-component is a separate cationic unit, the [Fe(bpca),]+, having a noncoordinated NO3- group, placed relatively close to the complex. The distance between the barycenters of the complex cation and nitrate anion is about 5 Å; the anion having close contacts with atoms of the ligand wings, e.g. about 2.5 Å for a CH...O interaction, as can be seen in Fig. 1. The NO<sub>3</sub><sup>-</sup> counter ion, though not coordinated, is not completely free, being involved in the hydrogen bonding established with the lanthanide units (vide infra the discussion related to the Table 2). The differences of [Fe(bpca)<sub>3</sub>]\* NO<sub>3</sub>\* couples among the crystallographic nonequivalent species are negligible.

The lanthanide sub-lattice shows a series of interesting peculiarities. The f complexes,  $[Er(H_2O)_4(NO_3)_3]$ , are neutral but show a visible polar building, because the negative ligands,  $NO_3$ , are separated in one hemisphere of coordination environment, whereas the aqua ligands are on the opposed side.

There are three crystallographic  $[Er(H_2O)_4(NO_3)_3]$  nonequivalent units, slightly different, as a consequence of the demands resulted from their fitting into a hydrogen bonded chain. The three units are practically collinear and consecutive along the chain. The chain incorporates

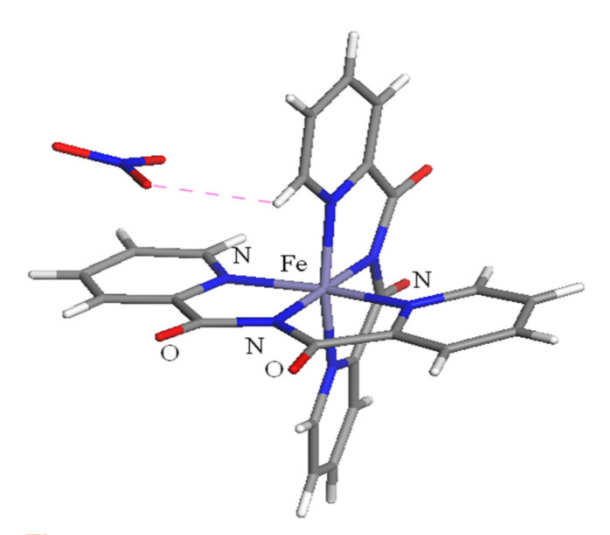


Figure 1. The complex cation and the nitrate counter ion in the [Fe(bpca)<sub>2</sub>][Er(NO<sub>3</sub>)<sub>3</sub>(H<sub>2</sub>O)<sub>4</sub>]NO<sub>3</sub> compound. The CH...O close contact of the nitrate and one ligand is figured as dashed line.

the inversion as symmetry element, allowing the continuation of the collinear pattern by repeating the three-membered sequence. In Fig. 2 one observes the sequence of three independent units marked by {1}, {2} and {3}, altogether with the continuation sequence resulted by inversion: {3'}, {2'} and {1'}, respectively. Certain NO<sub>2</sub> groups undergo disorder, probably of dynamic nature. We selected for representation and electron structure calculations certain conventional configurations, as is the case of unsymmetrical coordination of NO<sub>3</sub>-(2) ligands in the {1} and {3} units. These nitrates are practically mono-coordinated; the non-bonded end constructing intermolecular hydrogen bonds (with the aq, aqua ligand in the unit {1} and the aq, in unit {3}). The supramolecular bonding results from hydrogens of aqua groups of one sphere approaching the nitrate oxygen atoms of a proximal unit. In the sequence between the {2} and {3} units of the chain there are aqua ligands from neighbour lanthanide complexes binding the above mentioned non-coordinated, formally free, nitrate counter-ions.

The whole crystal has a layered aspect, the d units and f ones forming alternating 2D sub-assemblies, as can be seen in the Fig. 3. Practically, the hydrogen bonding glues the lattice: the lanthanide neutral units each to other and to the  $\mathrm{NO}_3$ - nominal anion. The free nitrato ligands are involved in CH...O weak bonding toward the ligands of the cation. Obviously, the ionic bonds contribute also, in varied ways: the direct cationanion Madelung stabilization, as well as dipole-dipole effects in the lanthanide sub-lattice or the ion-dipole effects from these components toward the cation and anion units.

#### 3.2 The bonding regime and assembling of lanthanide coordination units

The most interesting structural feature of the discussed system is found in its lanthanide part. In Fig. 2 one observes the assembling of lanthanide units in the chain and the labeling of each ligand inside its own coordination sphere. For better comparability, in Fig. 4 the units are represented individually and rotated to obtain similar mutual orientation. The units are roughly similar, having the above noticed polar structure, with NO<sub>3</sub>- ligands at one side and the water ones on the opposite part. If the nitrate ligands are conventionally placed with their barycenters in the xy plane (i.e., the sheet plane in the Fig. 4) then the water fragments are placed in the xz middle plane. The ligands labeled NO<sub>3</sub>-(1) and NO<sub>3</sub>-(2) are axially opposed in all the units. Therefore the dipole moment of the molecule is oriented

approximately along the line between the NO<sub>3</sub>-(3) ligand and the lanthanide site. The units (1) and (3) are the most matching in mutual similarity, the fragment (2) having a slightly different topology of the nitrato ligands.

For a systematic insight in the structure of the lanthanide chain we will analyze first the forces behind the coordination process. In this view, the ADF package offers interesting tools, allowing the estimation of the formation energy with respect of predefined fragments [20]. Thus, taking the lanthanide ions and each nitrate and water molecules as preliminary computed fragments, one finds the total energy of formation from the metal ion and the seven ligands. To estimate the binding energy of each individual ligand, the implied fragments are the given ligand and the remainder of the complex (the metal ion with the other six ligands, as predefined unit). The results are given in the Table 1.

It is interesting to note that the ligand binding energies from ADF decomposition are close to the simplistic electrostatic estimation obtained by taking as point charge the Mulliken populations of each atom. More specifically, taking the atoms A in a given ligand L, with their separation from central metal,  $R_{\scriptscriptstyle MA}$  in Ångstroms, the working formula is  $\sim 332 \cdot Q_M \sum q_A / R_{MA}$ where the numeric factor serves to yield the result in kcal mol<sup>-1</sup>, while  $Q_{\scriptscriptstyle M}$  and  $q_{\scriptscriptstyle A}$  are the Mulliken charges on metal and ligand atoms. This result suggests that the bonding in lanthanide units is practically noncovalent, effectively ionic. The conclusion must be submitted to more detailed analysis, since, in spite of the relative simple reasoning, the use of Mulliken charges brings implicit assumptions of quantum factors. It is rather difficult to fully rationalize the small mutual differences between the association energies of the ligands. For instance one may observe that the association energies of the NO<sub>3</sub>-(3) ligand are smaller than the other ones, except the case of unit 3 in the DFT results and the unit 2 in the electrostatic estimation. The smaller stabilization, as averaged trend, of the third nitrate can be explained by the fact that this ligand faces the direct neighborhood of the two other negatively charged nitrates NO<sub>2</sub>-(1) and NO<sub>3</sub>-(3). In turn, the distant ligands of the NO<sub>3</sub>-(1) NO<sub>3</sub>-(2) couple undergo smaller mutual electrostatic repulsion, being both of them in direct neighborhood with one negative ligand, the NO<sub>3</sub>-(3) one. Another comparative rationalization can be proposed relating the larger DFT association energy of the NO<sub>3</sub>-(1) than those of NO<sub>3</sub>-(2) with the the simpler electrostatic estimation of the association energy.

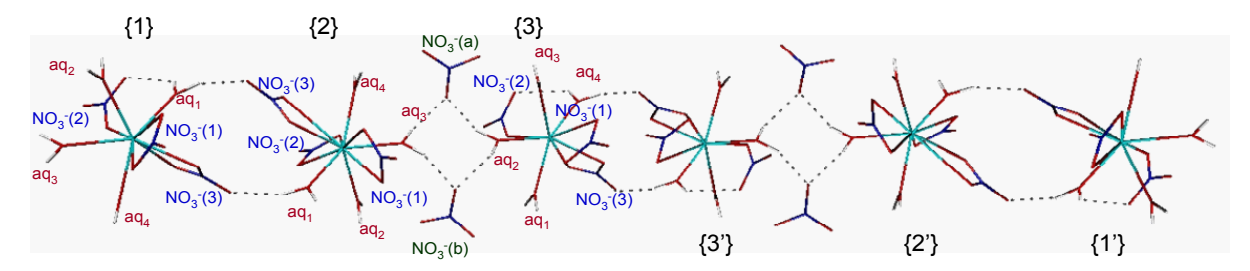


Figure 2. The chained sequence of three crystallographic nonequivalent [Er(NO<sub>3</sub>)<sub>3</sub>(H<sub>2</sub>O)<sub>4</sub>] units, labeled {1}, {2}, {3}. The next three units, {1'}, {2'}, {3'} are in symmetry relationship, via inversion. One observes the linear placement of the lanthanide sites along the hydrogen bonded chain. The ligand and unit labels serve for corresponding further identification in Fig. 4, Table 1 and related discussion.

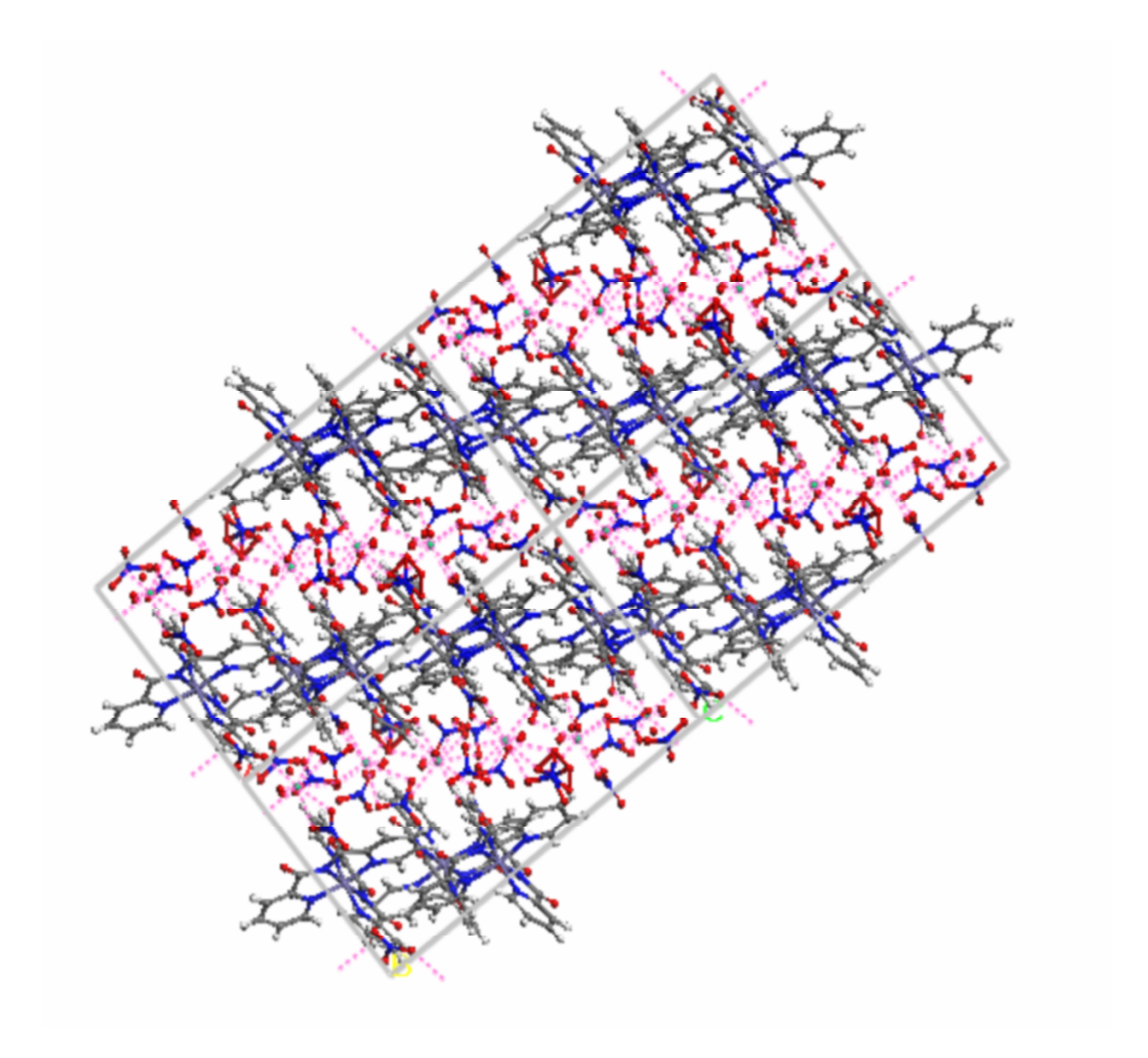


Figure 3. The general structure of the [Fe(bpca)<sub>2</sub>][Er(NO<sub>3</sub>)<sub>3</sub>(H<sub>2</sub>O)<sub>4</sub>]NO<sub>3</sub> crystal. The view along the b axis of the expanded content of 8 elementary cells. The orientation illustrates the layered constitution, in d and f alternating 2D shells.

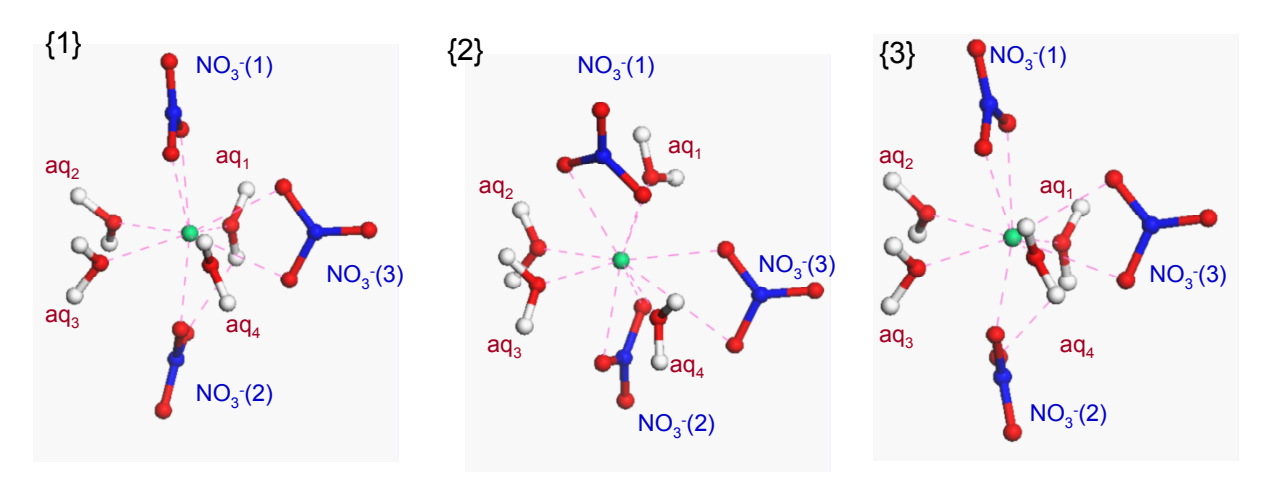


Figure 4. The three different lanthanide complexes units, conventionally oriented to illustrate their similarity. The labels of the ligands correspond to those in Table 1.

Table 1. Binding energies of the ligands in each of the three independent f units. The left half contains the full DFT quantum result from ADF energy decomposition procedures. The left side contains the estimation after taking the Mulliken populations as point charges into a Coulomb formula (interaction between lanthanides and point charges on atoms of the given fragment). All quantities are in kcal mol<sup>-1</sup>.

[Lu(H <sub>2</sub> O) <sub>4</sub> (NO <sub>3</sub> )		DFT computed formation energy, with fragment based methods from ADF			Point charge estimation of electrostatic energy (with Mulliken charges)		
	{1}	{2}	{3}	{1}	{2}	{3}	
H,O(1)	-20.0	-14.2	-13.5	-17.8	-15.0	-17.3	
H,O(2)	-18.9	-11.5	-4.2	-17.9	-14.3	-16.3	
H <sub>3</sub> O(3)	-12.6	-12.8	-9.7	-16.4	-14.7	-15.5	
H <sub>2</sub> O(4)	-22.6	-15.2	-18.3	-15.4	-13.8	-13.9	
NO <sub>3</sub> -(1)	-155.1	-154.2	-145.5	-146.2	-147.7	-146.9	
NO <sub>3</sub> -(2)	-153.4	-145.9	-132.6	-149.6	-143.1	-157.9	
NO <sub>3</sub> -(3)	-138.5	-113.6	-133.8	-137.3	-145.1	-138.9	

The mono-coordination is determined by the apparent disruption of the chelation after the formation of an inner hydrogen bond. The pure electrostatic part does not represent well the effects implied in the hydrogen bonding contribution.

The ADF fragment formation energies were estimated also for the dimer sequences, calculated at the experimental geometries from the 1D lanthanide sublattices. This procedure estimates the supramolecular assembling energies. For this purpose, the preliminarily computed monomers are used as building fragments. The results in Table 2 show, aside the total bonding (association) energy, its dichotomization in the components: Pauli repulsion, electrostatic energy and orbital part [25].

The dimer sequence made by the {1} and {2} units is slightly bonded by about -0.5 kcal mol<sup>-1</sup>. The contributors are the electrostatic forces, of dipolar nature, and the hydrogen bonding that can be related to the weak orbital stabilization. Since the balance of electrostatic attraction vs. Pauli repulsion left only a small negative energy in favor of the association effect, one may say that the contribution of hydrogen bonding is decisive

for the supramolecular binding. The {2}+{3} sequence made without the involvement of non-coordinated  $NO_3$ - groups (labeled  $NO_3$ -(a) and  $NO_3$ -(b) in the Fig. 2) appears as unstable (positive formation energy). Here the electrostatic interaction is unfavorable since, eliminating the lattice nitrate ions, the protons prepared for making hydrogen bonds with these groups, point now, at distance, to each other. The orbital component is weaker because of a larger separation between the {2} and {3} lanthanide centers, as compared to the {1}+{2} pair. The intercalation of the lattice anions into computed models yields a firm stabilization of about -2.3 kcal mol-1, assignable to the newly created hydrogen bonds and ion-dipole interactions (*i.e.*, charged nitrate vs. neutral lanthanide complexes).

It is interesting to correlate the architecture of supramolecular association with the orientation of computed dipole moments of each unit, considering their ( $\mu_X$ ,  $\mu_y$ ,  $\mu_z$ ) vectorial components. With a conventional overall rotation, to have the dipole moment of unit {1} aligned to the z axis, (0.00, 0.00,9.02) D, the vectors for the {2} and {3} moieties are (0.57, 6.36, -9.44) D and (-1.55, -2.24, 8.43) D, respectively. One observes that

**Table 2.** Analysis of the intermolecular association energies in the dimer sequences. All quantities are in kcal mol<sup>-1</sup>.

Intermolecular Association	{1}+{2}	{2}+{3}	{2 & 3}+2NO <sub>3</sub> -
Total Bonding	-0.48	0.32	-2.32
Pauli Repulsion	0.66	0.03	2.75
Electrostatic Energy	-0.7	0.34	-3.1
Orbital Stabilization	-0.43	-0.05	-1.97

the dipoles take alternately opposed, approximately anti-parallel orientations, having the main component (z in our case) with alternating sign (i.e.,  $\mu_z = +9.02$ , -9.44 and 8.43). The alternation continues along the chain because of the inversion symmetry at the contact between the {3} and {3'} units (see Fig.1), i.e., the {3'} will have the (1.55, 2.24, -8.43) D dipole vector. With respect to the mean axis passing between the {1}, {2}, {3} centers, the orientation of dipoles in these units can be evaluated as, ~ +160°,~ -30°,~ +155°, respectively. The approximate inversion of dipoles along the {1}-{2} and {2}-{3} contacts illustrate that these pairs are somewhat close to an inversion-like relationship, even though they do not obey such strict symmetry. The loss of local potential symmetry can be interpreted as a cost for the formation of extended chain structure.

# 3.3 Idealized models of stereochemistry and bonding in the lanthanide coordination units

The investigation is continued by approaching the geometry optimization, to check whether the actual monomer structures are, in the major aspects of the building, the result of their encapsulation in the supramolecular assembles or it also responds to a local optimal criterion. Certain conclusions can be drawn in examining Fig. 5, the structures obtained as absolute and local minima, starting with different topologies of initial idealized geometries. The geometry most similar to the experimental structures is that labeled {A} in Fig. 5. It corresponds to the absolute minimum, confirming the fact that the stereochemistry of lanthanide units is primarily the subject of the forces exerted at the local molecular level. The supramolecular stage determines only slight distortions of ligands positions and orientation on each coordination sphere, to meet also the demands of establishing further contacts by intermolecular hydrogen bonds.

The idealized {A} unit has  $C_{2v}$  symmetry. The {B} unit has also  $C_{2v}$  symmetry, but has undergone (by initial design of the starting geometry) a rather drastic mutation, by the rotation with 90° of all the chelating  $NO_3$ - groups. The {C} structure has no symmetry, being designed initially as imbrication of a trigonal  $Ln(NO_3)_3$ 

tris-chelate pattern with a square planar set of water molecules. The {B} and {C} are higher in energy than {A} by the relatively small quantities 12.23 kcal mol-1 and 8.62 kcal mol-1, respectively, probing the rather floppy nature of the lanthanide coordination sphere, with low barriers between rather drastic rearrangement of the ligands. The {C} looks somewhat similar to the more distorted experimental unit {2}, while {A} is quite close to the {1} and {3} ones. The experimental units are about 20 kcal mol-1 higher in energy compared to the idealized {A} structure, a small departure that certifies the choice of the idealized C2 stereochemistry as the optimal structure of stand-alone monomers. The reported energies, as well as the detailed geometry parameters, should be taken in semiquantitative respect, because we are using in computation the Lu(III) diamagnetic ion instead of the more problematic Er(III) ion. The geometries of Er(III) and Lu(III) analogues are expected to be slightly affected by the so-called lanthanide contraction effect [26]. However, because Er(III) is quite close to the Lu(III) in the periodic table, the effect is small, involving about 3% changes in the ionic radii. Confined to the averaged quantities, the Ln-O distances are 2.57 Å for nitrate and 2.36 Å for agua ligands (taken over the three experimental units), compared to the 2.42 and 2.48, respectively in the {A} unit. The comparisons are quite close in semiquantitative sense, considering on one hand, all the complex factors involved in the idealization process and, on the other, the fact that the experimental geometries respond also to the supramolecular demands. The experimental average is higher because it involves certain distortions of the nitrate chelate coordination (see, e.g., ligand NO<sub>3</sub>-(2) in unit {1}), the ligand becoming mono-dentate due to intramolecular hydrogen bonding effects. For the aqua ligand the computation brings a small overestimation, reasonable in the invoked circumstances, particularly under the provision that not such details are the focus of the present investigation. Given the reasonable qualitative and semiquantitative comparability of the optimized molecular structures with the experimental ones, we will proceed to a detailed analysis of the bonding regime, taking in this case the {A} idealized unit. The calculation of coordination energies will be repeated for the idealized unit, detailing also the corresponding elements. The Table 3 shows the computed energies, taken for the binding of the full set of the seven ligands and also for each individual ligand.

A quite intriguing fact is that the orbital stabilization is smaller in module than the Pauli repulsion. The Pauli repulsion is a term of pure quantum nature that appears between the closed shell subsystems [27]. It is similar to the force that prevents the formation of

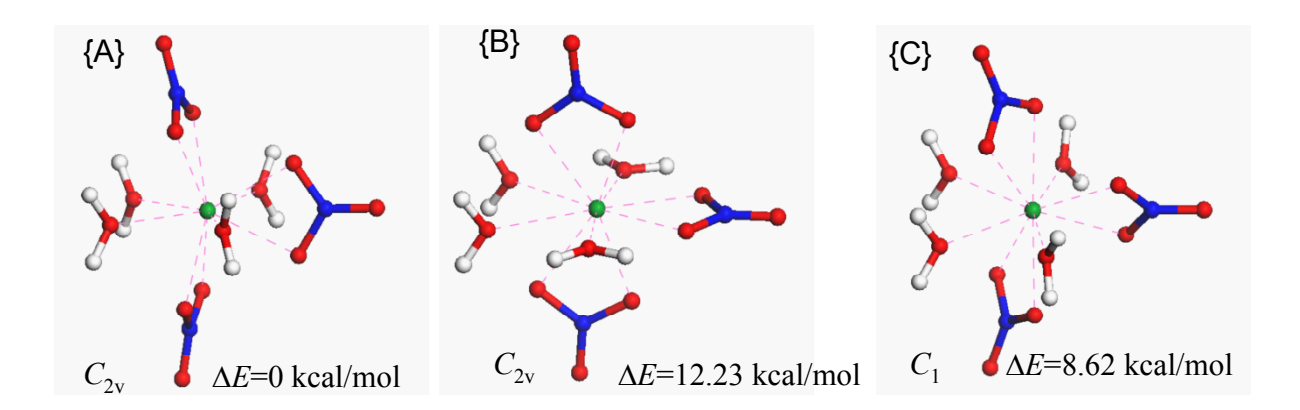


Figure 5. Different structures corresponding to absolute, {A}, and local minima, {B} and {C}, from DFT geometry optimization of the [Lu(H,O),(NO,),] model monomers. The relative energies and point group symmetries are marked below each molecular picture.

the molecules between noble gas atoms. The quantity shell, in line with the suggestion from the Mulliken Table 3. The formation (coordination energies) related to the full set o ligands (first column) and each of symmetry independent ligands (next columns) for the idealized {A} structure.

Formation energy	3xNO <sub>3</sub> - + 4xH <sub>2</sub> O	NO <sub>3</sub> -(1) <u>≡</u> NO <sub>3</sub> - (3)	NO <sub>3</sub> -(2)	$H_2O(1)\equiv H_2O(4)$	$H_2O(2)\equiv H_2O(3)$
Total Bonding	-1086.5	-149.61	-144.22	-13.37	-10.09
Pauli Repulsion	301.47	70.48	79.71	33.1	30.18
Electrostatic Energy	-1148.25	-235.59	-227.62	-45.86	-42.52
Total Orbital	-239.72	15.51	3.69	-0.6	2.25

labeled as orbital stabilization can be assigned to the covalence effects. More precisely, the effective energy of covalence can be interpreted as the amount remained after the summation of the generally opposed Pauli and orbital terms. Generally this is a negative value, marking the role of covalence in binding. However, in our case the repulsion dominates, suggesting the conclusion that the bonding of the ligands is a noncovalent process, effectively determined by the electrostatic forces.

On the other hand, a certain role of the metal-ligand overlapping can be detected, due to the fact that the Mulliken population analysis yields a supplement of about 1 electron in the 5d shell of the lanthanide ion. This result suggests the role played by this formally empty shell in accepting an electron density donated by the lone pairs of the ligands. In order to assess the energies involved in donor-acceptor effects we proceeded to a series of numerical experiments, applying the enforced elimination of certain sets of virtual orbitals from Ln(III) or NO<sub>2</sub> and H<sub>2</sub>O ligand fragments. This is possible by dedicated keywords of the ADF code [28]. Table 4 shows in the first line the energy shifts for the total energy of formation from Lu(III) and the separated seven ligands, at the progressive elimination of the virtual fragment orbitals. Comparing the energy growth at the elimination of the s, p and d empty orbitals on Lu(III) one notes that the most important role in the bonding belongs to the d

population analysis. One notes a certain symbiotic effect, since the energy shift at the combined elimination of sd or spd shells is a bit larger than the sum estimated with the shifts from pure shell removals. The calculations suggest that the empty d AOs work as acceptors of the densities offered by occupied ligand MOs. The computational experiment involving the removal of all virtual MOs on all the ligands shows that the apparent back-donation, from metal to ligand, is also a factor of bonding also, the shift being about 60 kcal mol<sup>-1</sup>, *i.e.*, comparable with the quantity resulting from the d-shell removal.

Table 4 offers also the charge assignable to the fragments according to the Mulliken and Hirshfeld population analyses [29]. For the full system (without no virtual removal) the Mulliken charge at lanthanide is +1.73, the nitrates being negatively charged from -0.63 to -0.66, and aqua ligands practically neutral, with 0.05. The Mulliken analysis is a conventional formula, which is not appropriate for polar or ionic systems since it performs the equal sharing of overlap density toward the partners of different electronegativity (metal ion and ligand in our case). In such cases, the Hirshfeld analysis is more appropriate [29-30], since it performs the partition according to the initial contribution of the unperturbed fragments to the density in a given point of molecular space.

**Table 4.** Numerical experiments at systematic removal of the fragment virtual orbitals from Ln(III) (s, p, d shells) and/or from ligands (all virtuals from all ligands). The shift of total bonding energy (with respect of formation from lanthanide and seven ligand fragments) and the fragment charges according to Mulliken and Hirshfeld analyses.

Eliminated virtual orbitals	s	р	d	sd	spd	ligands	sd and ligands	spd and ligands
Bonding energy shift								
ΔE (kcal mol <sup>-1</sup> )	2.99	4.44	91.79	97.63	102.79	67.12	210.88	227.3
Mulliken Charges								
Lu(III)	1.77	1.90	2.55	2.70	2.96	1.98	2.68	2.92
$NO_{3}^{-}(1) \equiv NO_{3}^{-}(3)$	-0.68	-0.71	-0.85	-0.88	-0.94	-0.78	-0.93	-0.98
NO <sub>3</sub> -(2)	-0.63	-0.68	-0.86	-0.89	-0.97	-0.74	-0.93	-0.98
$H_2O(1)\equiv H_2O(4)$	0.06	0.05	0.00	-0.01	-0.03	0.08	0.03	0.01
$H_2O(2)\equiv H_2O(3)$	0.05	0.05	0.00	-0.01	-0.03	0.08	0.03	0.01
Hirshfeld Charges								
Lu(III)	2.55	2.55	2.92	2.94	2.96	2.52	2.99	3.06
$NO_3^{-1}(1) \equiv NO_3^{-1}(3)$	-0.89	-0.89	-0.97	-0.98	-0.98	-0.90	-1.00	-1.02
NO <sub>3</sub> -(2)	-0.86	-0.86	-0.97	-0.98	-0.98	-0.85	-1.00	-1.01
$H_2O(1)\equiv H_2O(4)$	0.03	0.03	0.01	0.00	0.00	0.04	0.00	0.00
$H_2O(2)\equiv H_2O(3)$	0.02	0.02	0.00	0.00	-0.01	0.03	0.00	0.00

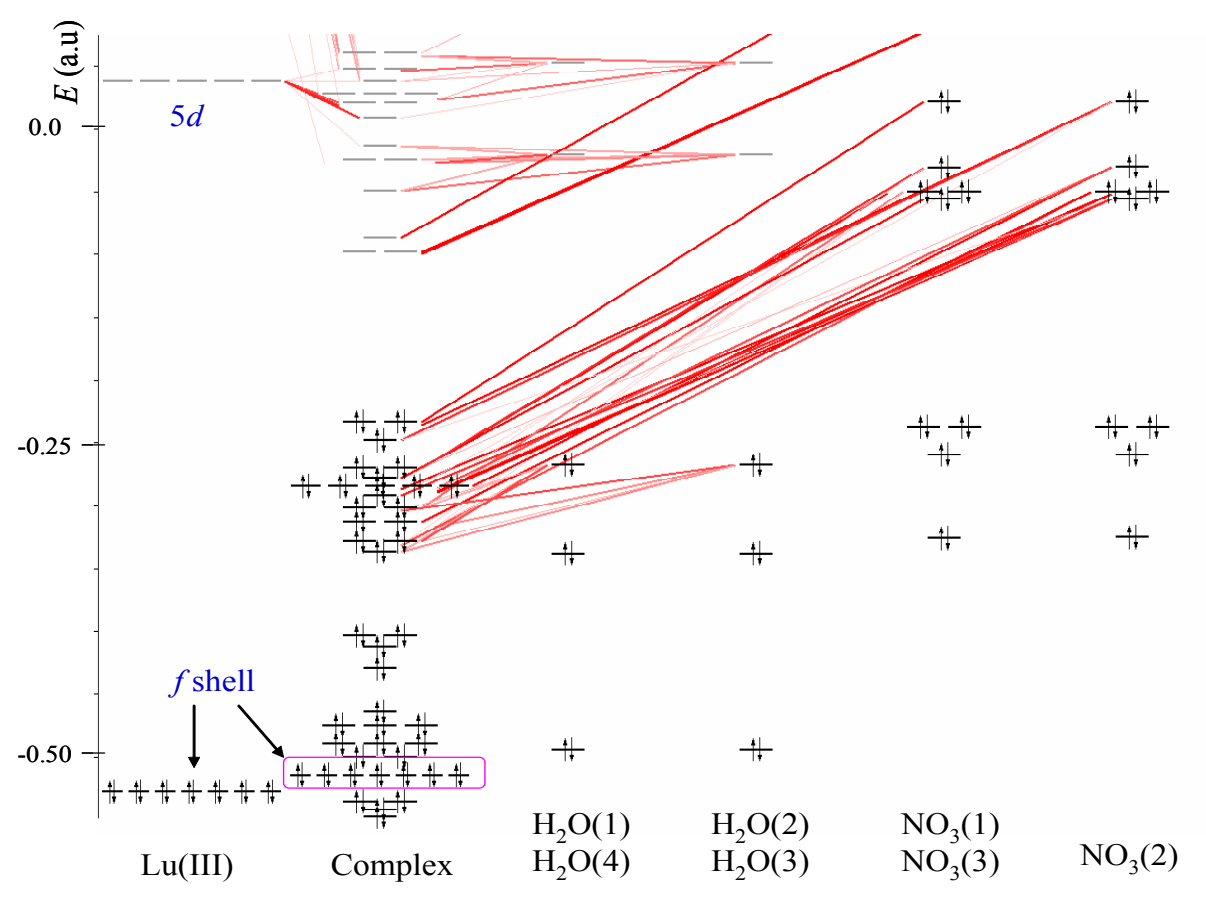


Figure 6. MO diagram of idealized [Lu(H<sub>2</sub>O)<sub>4</sub>(NO<sub>3</sub>)<sub>3</sub>] (i.e., {A} structure) and correlation with fragment orbitals. One observes the inner nature of the f shell and the ligand nature (marked by lines from MOs in the complex to corresponding fragment levels) of the upper sequence of occupied MOs.

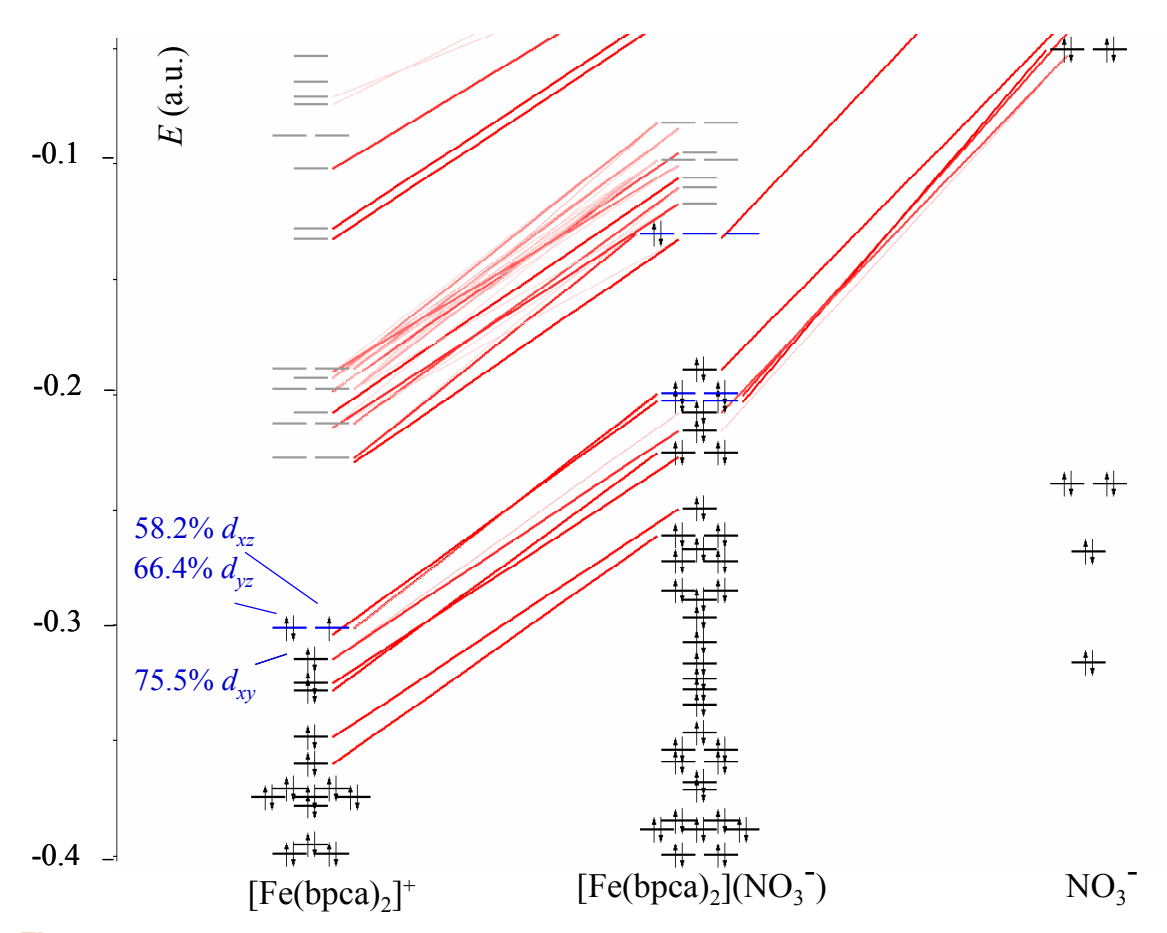


Figure 7. MO diagram of the [Fe(bpca)<sub>2</sub>](NO<sub>3</sub>) couple, taken at experimental geometry, drawn with respect of [Fe(bpca)<sub>2</sub>]+ and NO<sub>3</sub>- fragments. One observes the non-aufbau nature of the supramolecular electron structure and the accidental degeneracies of non-interacting distant MOs.

The Hirshfeld charge on the lanthanide of {A} complex is 2.54, closer to the nominal oxidation state III. For the nitrates it is close to the -1 charge (-0.89 for the equivalent  $NO_3^-$  (1) and  $NO_3^-$  (3), -0.85 for  $NO_3^-$  (2)), the aqua ligands being almost neutral with a charge of 0.02 to 0.03 for the two symmetry species. With the progressive elimination of the virtual shells the changes in both Mulliken and Hirshfeld charges evolve toward the nominal +3 and -1 on the lanthanide and nitrate, likely due to the elimination of donation and back-donation effects. However, a certain donor-acceptor activity still exists in the complex, in spite of the fact that the covalence is ineffective, being surpassed by the quantum exchange effects comprised in the Pauli repulsion.

Finally, the electron structure of the lanthanide complex will be considered with the help of the MO diagram in Fig. 6. This shows that the f shell is confined at very low energies, having many ligand-type orbitals above, whereas the frontier MOs are made of practically non-interacting lone pairs of the ligands. Having such a placement of the f shell, the paramagnetic analogues,

*i.e.*, the Er(III) complex, will show a non-aufbau structure with unpaired electrons in the deep f shell, below many doubly occupied MOs. Even with programs affording in principle the imposing of non-aufbau structures and fractional orbital populations, such as ADF, this situation gives rise to severe convergence problems, as proved by our tests on this issue.

# 3.4 The d-type coordination unit and the features of the bpca- ligand

In this section we will comparatively analyze the coordination inside the d complex unit and its further intermolecular long range interaction with the nitrate counter ion. The formation energy of the d-type coordination unit from the Fe(III) and the two bpcaligand is about -1400 kcal mol<sup>-1</sup>. The amount per ligand is half this quantity, -700 kcal mol<sup>-1</sup>, sensibly higher compared to the association of the ligands in the

**Table 5.** The energy decomposition in components for the coordination bonding inside the d-type cation and its intermolecular association with the lattice nitrate counterion.

_	Computed System	[Fe(bpca)₂]⁺	[Fe(bpca) <sub>2</sub> ](NO <sub>3</sub> )		
	Fragments	Fe <sup>3+</sup> + 2bpca <sup>-</sup>	[Fe(bpca) <sub>2</sub> ]++NO <sub>3</sub> -		
	Total Bonding	-1454.23	-47.30		
	Pauli Repulsion	537.48	13.87		
	Electrostatic Energy	-1105.26	-67.34		
	Orbital Stabilization	-886.45	6.16		

lanthanide units. The decomposition shows also that in this case we have a firm predominance of the orbital stabilization against the Pauli repulsion. The electrostatic term is also large, allowing the qualitative conclusion that the coordination follows a partly covalent - partly ionic regime.

The coordination sphere shows no real symmetry element, but it is roughly close to the  $\rm D_{2d}$  point group with the main axis passing through the amide-type nitrogen atoms of each ligand. If we assign this line to the z axis, we may specify the contribution of the d AOs in the last three occupied MOs: 75.5%  $\rm d_{xy}$ , 66.4%  $\rm d_{yz}$ , 66.1%  $\rm d_{xz}$ , where the first two levels are doubly occupied and the last one has an unpaired electron. This is in line with a low spin d⁵ configuration, having the subset of  $\rm t_{2g}$ -type orbitals occupied. These MOs are in line with a Ligand Field scheme. The relative high content of the ligands in the frontier MOs (with percentages that remain of the above mentioned d contents, divided equally between the two ligands) illustrates the involvement of covalence in the coordination bonding.

The second column of Table 5 gives the energy analysis for the long range interactions between the complex cation and the anion. One notes that this is a

noncovalent, practically ionic, effect. It is interesting to note that the calculation itself is not trivial, in spite of the apparent simplicity. The orbital diagram of the  $[Fe(bpca)_2]$   $(NO_3)$  couple, drawn with respect of its molecular components show a non-aufbau aspect of the frontier orbitals. There are several accidental degeneracies of non-interacting orbitals from the different units. Several doubly occupied MOs of the nitrate are placed a bit higher than the partly filled  $t_{2g}$ -like subset of the complex cation.

#### 4. Conclusions

We analyzed here the stereochemistry and electron structure of [Fe(bpca)<sub>2</sub>][Er(NO<sub>3</sub>)<sub>3</sub>(H<sub>2</sub>O)<sub>4</sub>]NO<sub>3</sub>. The relative complexity of the different coordination and supramolecular association modes was decrypted with the help of properly designed post-computation analyses and numeric experiments. In this way, we advanced toward the understanding of the mechanisms acting in the supramolecular chemistry of coordination units, going beyond the usual qualitative description of crystal architectures and taxonomic account of long range contacts.

## **Acknowledgements**

We gratefully acknowledge the financial support of CNCSIS, the Romanian National University Research Council (PN2-ID-PCE grant no 467/2009). MC is indebted to Alexander von Humboldt Foundation for supporting this material as invited talk at Humboldt Conference on Noncovalent Interactions, October 22-25, 2009, Vrsac, Serbia.

#### References

- [1] L. Maretti et al., Inorg. Chem. 46, 660 (2007)
- [2] T. Kajiwara et al., Inorg. Chem. 45, 4880 (2006)
- [3] J. Paulovic, F. Cimpoesu, M. Ferbinteanu, K. Hirao, J. Am. Chem. Soc. 126, 3321 (2004)
- [4] M.Ferbinteanu et al., J.Am. Chem. Soc. 128,9008 (2006)
- [5] M. Ferbinteanu et al., Solid State Sciences 11,760 (2009)
- [6] M. Ferbinteanu et al., Polyhedron 26, 2069 (2007)
- [7] P. Caravan, J.J. Ellison, T.J. McMurry, R.B. Lauffer, Chem. Rev. 99, 2293 (1999)
- [8] S. Cotton, Lanthanide and actinide chemistry (John Wiley & Sons, New York, 2006)
- [9] C. Benelli, D. Gatteschi, Chem. Rev. 102, 2369 (2002) and references therein

- [10] O. Kahn, Acc. Chem. Res. 33, 647 (2000)
- [11] J.P. Sutter, M.L. Kahn, O. Kahn, Adv. Mater. 11, 863 (1999)
- [12] M. Sakamoto, K. Manseki, H. Okawa, Coord. Chem. Rev. 219–221, 379 (2001) and references therein
- [13] C.M. Zaleski, E.C. Depperman, J.W. Kampf, M.L. Kirk, V.L. Pecoraro, Angew. Chem. Int. Ed. 43, 3912 (2004)
- [14] A. Mishra, W. Wernsdorfer, K.A. Abboud, G. Christou, J. Am. Chem. Soc. 126, 15648 (2004)
- [15] J.-P. Costes, F. Dahan, W. Wernsdorfer, Inorg. Chem. 45, 5 (2006)

- [16] P. Nockemann, B. Thijs, N. Postelmans, K. Van Hecke, L. Van Meervelt, K. Binnemans, J. Am. Chem. Soc. 128, 13658 (2006)
- [17] S. Tanase, J. Reedijk, Coord. Chem. Rev. 250, 2501 (2006) and references therein
- [18] D.J. Newman, B.K.C. Ng, Crystal Field Handbook (Cambridge University Press, Cambridge, 2000)
- [19] ADF 2006.01, SCM, Theoretical Chemistry, Vrije Universiteit, Amsterdam, The Netherlands, http://www.scm.com
- [20] G. te Velde et al., J. Comput. Chem. 22, 931 (2001)
- [21] C. Fonseca Guerra, J.G. Snijders, G. te Velde, E.J. Baerends, Theor. Chem. Acc. 99, 391 (1998)
- [22] A.D. Becke, Phy. Rev. A 38, 3098 (1988)
- [23] J.P. Perdew, Phys. Rev. B 33, 8822 (1986)
- [24] J.P. Perdew, Phys. Rev. B 34, 7406 (1986)

- [25] C.E. Dykstra, G. Frenking, K.S. Kim, G.E.Scuseria, Theory and Applications of Computational Chemistry (Elsevier B.V., Amsterdam, 2005) 291
- [26] F.A. Cotton F.G. Wilkinson, Advanced Inorganic Chemistry, 6th edition (John Wiley, New York, 1999) 1108
- [27] O.V. Gritsenko, P.R.T. Schipper, E.J. Baerends, Phys. Rev. A 57, 3450 (1998)
- [28] the RemoveFragOrbitals keyword, online documentation in http://www.scm.com/Doc/, Doc2009.01/ADF/ADFUsersGuide/page88.html
- [29] F.L. Hirshfeld, Theoretica Chimica Acta 44, 129 (1977)
- [30] C. Fonseca Guerra, J.-W. Handgraaf, E.J. Baerends, F.M. Bickelhaupt, J. Comput. Chem. 25, 189 (2004)